

A Cell Method Model for Sintered Alloys

Francesca Cosmi¹

Abstract: In industrial applications, microstructure inhomogeneities can derive from the manufacturing process and the final mechanical properties of the material depend on the resulting, complex, structural pattern of the constituents. In this paper, Cell Method plane models in the elastic and plastic fields are presented and applied to predict the behaviour of four sintered alloys, where the spatial arrangement of voids within the base material contributes to determine the mechanical behaviour. Unlike the Finite Elements and other methods, the Cell Method is a numerical method based on a direct discrete formulation of equilibrium equations, so that no differential formulation is needed in order to write the balance equations. One of the consequences of the Cell Method direct discrete approach is that no restriction is imposed by differentiability conditions so that the characteristic length of the elementary cell in the discretization can be of the same order of magnitude of the heterogeneities of the structure. Therefore, the Cell Method appears to be particularly suitable to assess the mechanical behaviour of heterogeneous materials. The results of the computations show a very good agreement with the experimental data of the sintered alloys examined.

Keywords: Numerical methods, Cell Method, sintered alloys, mechanical properties.

1 Introduction

A wide class of materials exhibits a complex structure at the micro-scale. The spatial arrangement of the constituents determines the local mechanical properties which in turn influence the final resistance of the whole specimen. This is true for numerous materials, ranging from biological tissues such as, for example, trabecular bone, to materials employed in industrial applications, sintered alloys and composites among them. In the latter case, microstructure heterogeneities either can derive from the manufacturing process or be added on purpose.

¹ DIMN, University of Trieste, Trieste, Italy, cosmi@units.it.

In all these instances, the final mechanical properties depend on the resulting phase pattern within the matrix. For example, porosity content and distribution strongly affect the mechanical properties by reducing the effective section and inducing stress concentrations in sintered alloys, which are obtained by joining together small particles of metal by applying heat at temperatures below the melting point. The outcome is a reduction of strength and ductility with respect to the wrought material, as shown for example in Fig. 1).

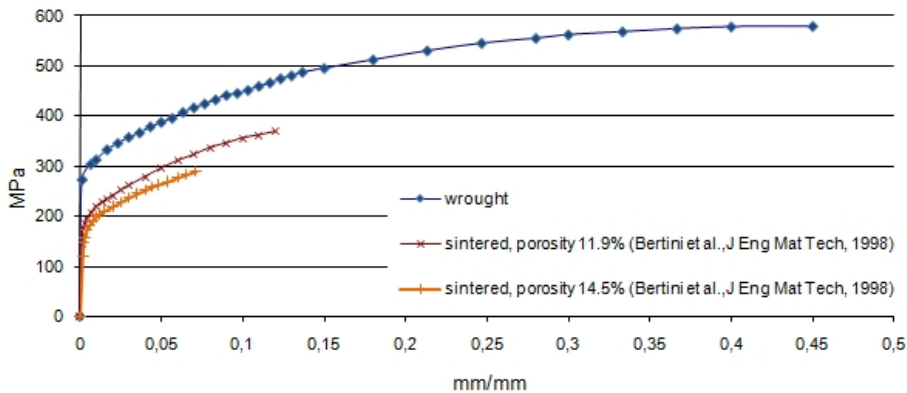


Figure 1: Tensile behavior of AISI316L steel and of two sintered alloys obtained from AISI316L powder.

The macroscopic direct numerical simulation of a microscopically heterogeneous engineering structure is virtually impossible. The numerical models used for computational material testing compute the average material properties on a statistically representative volume of the material (RVE). This homogenization process yields results that can in turn be used in macro-scale models (Fig.2).

Analytical models usually have a simple formulation but are based on parameters that do not have a clear physical meaning and must be calibrated by experimental tests. They cannot anticipate the behavior of a complex structure material and cannot be used to decide a micro-structure in order to meet predetermined macro-structural requirements.

In alternative, numerical models can be developed, so that simulations can anticipate the mechanical behavior of materials with a complex structure, accelerating the optimization process of high performance new materials. The development of numerical models results in an important reduction of experimental tests and project development costs. Several homogenization numerical models based on the use of

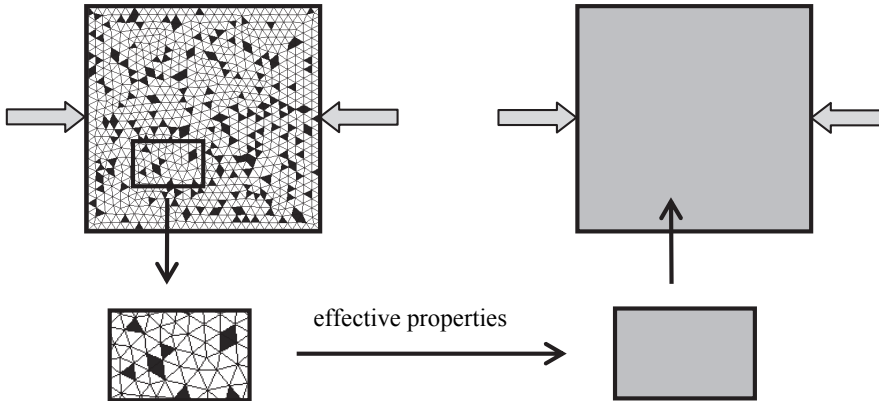


Figure 2: Estimate of effective properties for structural computations.

finite element method can be found in literature. They are essentially based on two approaches: the first generates a mesh in which the elements sides overlap with the internal interfaces of the material, while the second allows the possibility of discontinuities within a single element [Cannillo and Carter (2000), Zohdi and Wriggers (2001)].

For plane problems, the FEM approaches usually employ triangular or quadrilateral elements, often arranged in a periodic structure. The regularity of the resulting arrangement can be avoided by using alternative tessellation patterns, as in the Voronoi Cell Finite Element Method (VCFEM). These methods can be regarded as alternative FEM formulations and have been applied for computing the micro-structural properties of several types of materials [Ghosh and Mukhopadhyay (1991), Ghosh (2004), Grujicic and Zhang (1998)] and extended to include fracture models [Chao, Bai and Ghosh (2007)].

In this work, an entirely different approach is followed and plane models based on the Cell Method (CM) are applied to predict the mechanical behaviour of four sintered alloys in the elastic and plastic fields. The computations results show a very good agreement with experimental data.

2 Cell Method

The Cell Method is a recently developed numerical method, first introduced in [Tonti (2001)]. It has now been applied successfully in several fields ranging

through mechanics of structures, biomechanics, diffusion, dynamics, etc [Alotto, Grusso, Moro and Repetto (2008), Codecasa and Trevisan (2006), Cosmi (2011), Cosmi (2009), Cosmi and Dreossi (2007a), Cosmi and Dreossi (2007b), Cosmi and Hoglievina (2010), Cosmi, Steimberg, Dreossi and Mazzoleni (2009), Ferretti (2009), Ferretti, Casadio and Di Leo (2008), Heshmatzadeh and Bridges (2007), Straface, Troisi and Gagliardi (2006), Taddei, Pani, Zovatto, Tonti and Viceconti (2008), Zovatto and Nicolini (2007), Zovatto and Nicolini (2006)].

In general, the results obtained with the Cell Method are similar to the Finite Elements Method ones, but the two approaches are considerably different. Numerical methods like Finite Elements, Finite Difference, Boundary and Finite Volumes Methods all obtain the balance laws by introducing differential relations among the variables of the approximated field. All these methods require a two-step process: first, a differentiation to write the appropriate balance equations, then, a discretization of the equilibrium, differential, equations in order to solve the system. Thus, different discretization methods can lead to different sets of algebraic equations for the same mesh.

The Cell Method stems from the consideration that the geometrical information is lost in this two-step process and that, due to differentiation, part of the physics of the problem somehow vanishes in the formulation of the numerical problem. For example, derivability requirements impose restrictions on the field equations that are not related to the physics of the problem. The Cell Method, on the contrary, is based on a direct discrete formulation of the field laws and can be applied when variables cannot be differentiated, i.e. when the displacement field undergoes large variations or the heterogeneities dimensions are of the same order of magnitude as the mesh size. Since the focus of this work is on its applications, only a very brief description of the method, from an engineering point of view, is given in the following. The interested reader will find a detailed description of the Cell Method foundation and implementation in [Tonti and Zarantonello, (2009) and (2010)].

With the Cell Method, two geometrical complexes are used (Fig.3):

the *primal cells*, to which the *configuration* variables such as strain tensor, displacements, velocity are linked in the nodes;

the *dual cells*, which are the regions of influence of the nodes and on which the *source* variables, like stress tensor, forces, momenta, act. In this work, the barycentric complex associated with the primal cells was used.

2.1 Elastic field

Assuming a linear interpolation of the displacement field within the primal cells, strain components $\{\varepsilon\}_c$ and stress components $\{\sigma\}_c$ are uniform within the primal

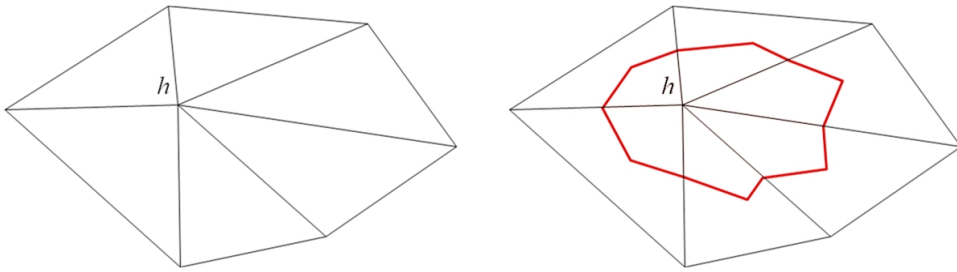


Figure 3: An example of possible primal cells and the corresponding region of influence in node h .

cell c :

$$\{\boldsymbol{\varepsilon}\}_c = [\mathbf{B}]_c \{u\}_c \tag{1}$$

$$\{\boldsymbol{\sigma}\}_c = [\mathbf{D}]_c \{\boldsymbol{\varepsilon}\}_c \tag{2}$$

where $\{u\}_c$ collects the nodal displacements, $[\mathbf{D}]_c$ represents the linear elastic constitutive law of the material and $[\mathbf{B}]_c$ describes the strain-displacement differential operator, fully similar to that of the Finite Element Method (FEM). However, the similarities with the FEM end here. In fact, the CM equilibrium equations are written directly in a discrete form for each region of influence, by adding up the contributions as outlined in Fig.4.

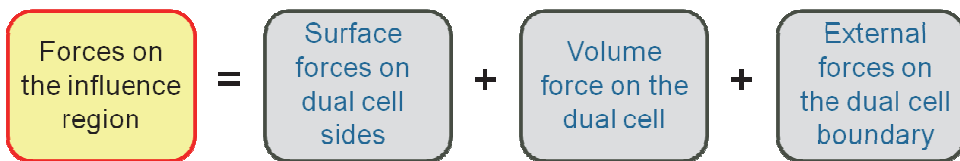


Figure 4: Balance equations framework.

An example of the forces on the sides of the influence region of node h in the cell c is shown in Fig.5.

For all the nodes of a primal cell c , the expression for the forces on the dual cell sides after some simple manipulation becomes $\{T\}_c = -tA_c [\mathbf{B}]_c^T [\mathbf{D}]_c [\mathbf{B}]_c \{u\}_c$, where A_c is the area and t is the thickness of the primal cell. The static balance of the influence region of node h can be then written as

$$\{T_h\} + \{F_h\} = 0 \tag{3}$$

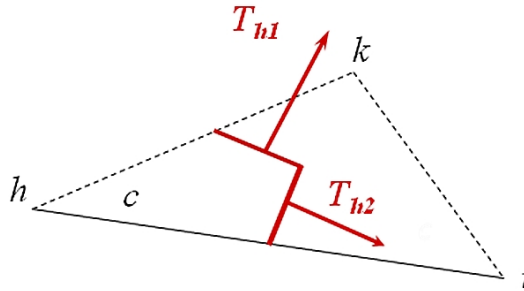


Figure 5: Forces on the sides of the region of influence of node h in the cell c .

where $\{T_h\}$ collects the forces on the sides and $\{F_h\}$ the volume and external forces of the dual cell. Combining eq. 3 for all the influence regions, a linear system is obtained and can be rewritten as

$$\{F\} = -\{T\} = [K]\{u\}. \tag{4}$$

It must be pointed out that, while it appears to be formally similar to that of FEM, the solving system has been obtained without using a differential formulation in order to write the equilibrium condition. Results indicate that accuracy, convergence rate and computing times are comparable (and sometimes even better than) with FEM [Cosmi (2001), (2005), (2008)]. Solution is directly obtained in the nodes with no extrapolation from super-convergent points and there is no locking, which greatly improves local stress evaluation in high gradient regions such as stress concentrations or hot spots.

2.2 Plastic field

Beyond the elastic point, in order to take into account the progressive damage accumulation that ductile materials exhibit when loaded, implementation of non-linear constitutive relationships is needed. An elastic-perfectly plastic incremental model for CM has been developed and discussed in [Nappi, Rajgelj and Zaccaria (2001)] and applied in [Cosmi (2004)]. For a more realistic simulation of real materials, in this work the model has been modified to include an elastic-plastic behaviour with linear hardening of the type shown for example in Fig.6.

For a plane state, the expression for the cell stress components now becomes $\{\sigma\}_c = [D]_c[\{\epsilon\}_c - \{\lambda\}_c] + [H]_c\{\lambda\}_c$, where $\{\lambda\}_c$ collects the inelastic strain components, uniform inside the primal cell consistently with the approximation used in the elastic field, and $[H]_c$ represents the linear constitutive law approximating the

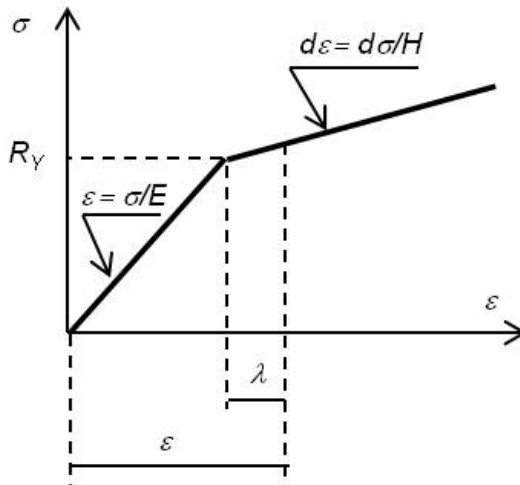


Figure 6: Example of uniaxial elastic-plastic constitutive law with hardening.

material behaviour in the second part of the stress-strain diagram. The load history is divided into a convenient number of finite steps. Displacements and internal stresses are known at the beginning of each step. The fundamental equation (4) in incremental terms now reads

$$\{\Delta F\} = [K] \{\Delta u\} - [L] \{\Delta \lambda\} \tag{5}$$

where $[L]\{\Delta \lambda\}$ collects the plastic strain equivalent forces. The condition $\{\Delta \lambda\} = 0$ is assumed at the first step and the system (5) is solved for $\{\Delta u\}$, so that also the stress components $\{\sigma\}_c$ and the deviatoric strain components $\{s\}_c$ can be computed in each primal cell. In this work, the Von Mises yield condition was assumed and the radius of the yield locus was used to update $\{\Delta \lambda\}$. The process is repeated until convergence is obtained, then a new step is considered.

Again, it can be noted that the Cell Method derives from a direct discrete formulation of physical laws. As a consequence, there are no limitations due to conditions of differentiability and the characteristic length of heterogeneities can be the same order of magnitude as the mesh size or the constitutive matrix can vary from one cell to the neighbor. These characteristics have been exploited in the application described in the following section.

3 Application: sintered alloys

The outcome of the simulations were compared with the corresponding experimental compression test results available in literature [Bertini, Fontanari and Straffellini (1998)]. Two different commercial powder materials were processed to attain two different residual porosity levels each. Alloys A1 and A2 were obtained from the pure iron NC100.24 commercial powder at a residual porosity level respectively of 13.4% (A1) and 9.8 % (A2), and the austenitic stainless steel AISI316L powder was processed to obtain alloy B1 with a 14.5 % and B2 with 12.04 % residual porosity levels. Given the variability of these materials, all experimental data published had been obtained as the average of 5 tests.

The mechanical properties of the constituent cells in the simulations were coherent with those of the corresponding powder materials and are reported in Table 1.

Table 1: Powder materials properties.

	NC100.24	AISI316L
E , elastic modulus in the first part of the stress/strain diagram (GPa)	207	197
R_y , yield stress (MPa)	180	275
H , tangential modulus in the second part of the stress/strain diagram (GPa)	2	3
ν_e , Poisson's ratio in the elastic field	0.3	0.3
ν_p , Poisson's ratio in the plastic field	0.5	0.5

For each model, a total of 1498 cells was used. The residual porosity was obtained by randomly distributing an adequate number n of "empty" cells among the cells of the constituent, as shown in Fig.7.

Empty cells are characterized by exhibiting a null stiffness. It can happen that a node is completely surrounded by empty cells, so that the stiffness of its influence region is totally null. In this case, the node displacement is set to null, thus avoiding singularity problems in the global stiffness matrix of the solving system. Since the contribution of this node to the elements of the local stiffness matrices is null by definition, this assumption does not alter the forces or the displacements in the system.

Similarly to the case of real alloys, porosity was made change slightly in a random way from one simulation to the other. Coherently with the experimental tests, the simulation results were computed as the average of 5 runs. The average number of empty cells in the model was 202 (± 20) for alloy A1, 147 (± 13) for A2, 216 (± 9) for B1 and 180 (± 17) for B2.

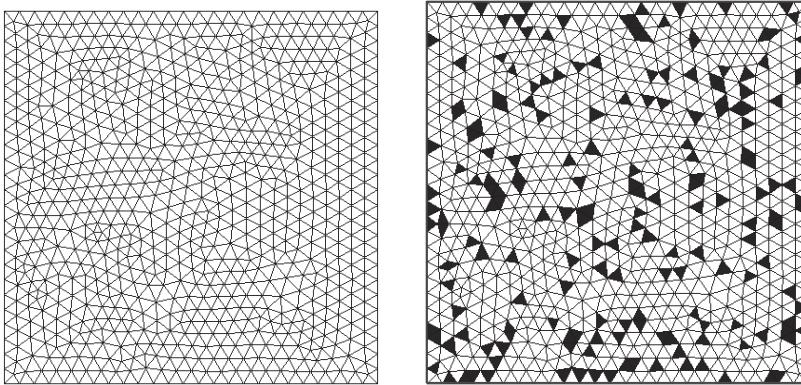


Figure 7: The mesh used in the simulations (left) and the empty cells (black) random distribution among the constituent cells (white) in one of the simulations of alloy A1.

3.1 Elastic field

The effective elastic moduli, E_{CM} , computed in the simulations, were compared with the experimental compressive Young moduli, E_S , available in literature. The results are shown in Table 2.

Table 2: Results in the elastic field.

Alloy	A1	A2	B1	B2
E_S (GPa)	150	168	140	150
E_{CM} (GPa)	161	175	152	160
Error	7 %	4 %	8 %	6 %

In all cases, the results obtained in the simulations indicate a very good agreement with experimental data. The percentual difference between the experimental and the numerical values remained well below 10%, which is considered the normal range of variability for these materials.

A plot of E_{CM} vs. porosity is shown in Fig.8. The values of the correlation coefficient for each data set are also reported in the same graph. It can be seen that porosity alone is not sufficient to account for all of Young's modulus variations although a general trend is present, confirming the effect of the microstructural arrangement of the component on the effective mechanical properties. As expected, for higher values of n/N , the variations in the spatial arrangement of the voids are more evident and this effect is more marked.

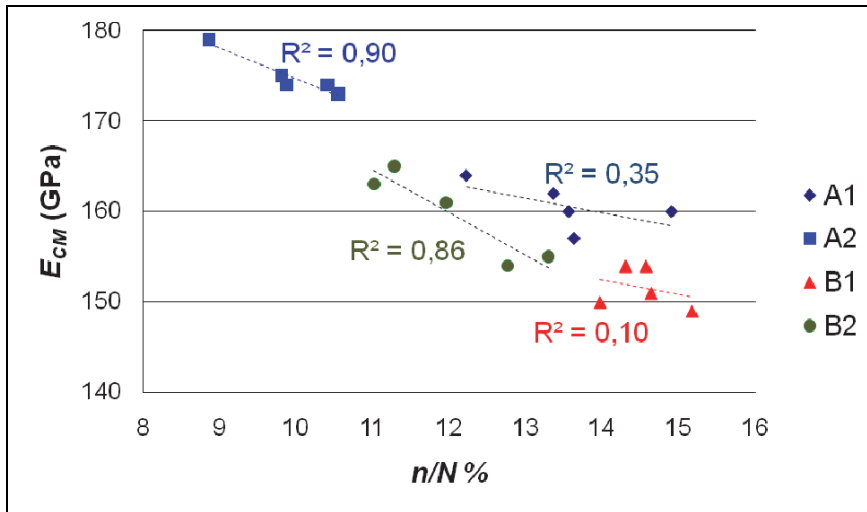


Figure 8: Computed effective elastic moduli E_{CM} (GPa) vs. porosity.

3.2 Plastic field

The mechanical behaviour of the modeled alloys has been simulated also beyond the elastic field, assuming a constitutive model with hardening for the ferrous cells. In the plastic region, the yield stress, the Poisson's ratio and the elastic modulus in the second part of the stress/strain diagram were assumed coherent with those of the corresponding wrought material and are reported in Table 1. Again, the simulation results refer to the average of the 5 runs. As an example, Fig.9 depicts the progressive plasticization at three different steps in one of the simulations (the model of Alloy A1 shown in Fig.7). Computing time was a couple of hours on a Intel Core™ i7 2.67 GHz based notebook.

The stress/strain plots obtained during the simulations of the four alloys are compared in Fig. 10 with the corresponding experimental diagrams. In general, it can be said that the simulation results reproduce well the compressive behaviour obtained in the experimental tests. In particular, the stress/strain plots of experimental data for these alloys show a discontinuity in the region of yielding, particularly interesting for industrial applications, and this behavior is well reproduced in the simulations, where the slope changes at yield.

The mechanical behavior of sintered alloys in the plastic field is often represented by Hollomon's equation, which is not suitable in the elastic region and is not able to reproduce for the above-mentioned discontinuity. For comparison, Hollomon's

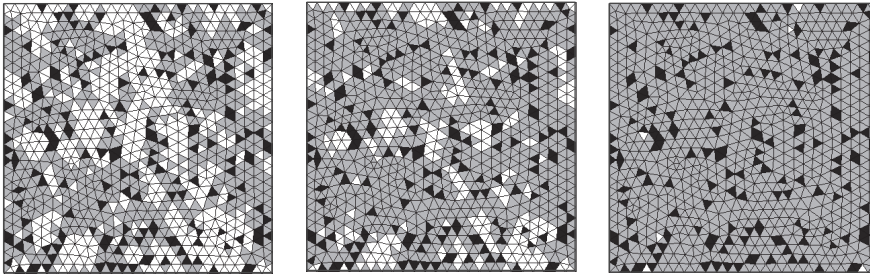


Figure 9: Progressive plasticization in a simulation (model of alloy A1 shown in Fig.7). The plasticized cells appear grey. The cells still in the elastic field are shown white, the void cells black.

equation is also plotted in Fig. 10, using the parameters given in [Bertini, Fontanari and Straffellini (1998)] that best fit the experimental data for the alloys.

It can be pointed out that analytical formulations such as Hollomon's equation cannot be used to predict the alloy behavior at a material design stage. In fact experimental tests are needed in order to tune the parameters involved, which have no physical meaning and can be therefore set only *a posteriori*. On the contrary, the Cell Method numerical simulations, based only on physical parameters such as the mechanical properties of the base material and the residual porosity levels, were able to predict the behavior of the sintered alloys with very good accuracy.

4 Conclusions

A numerical model suitable for the assessment of the mechanical behavior of sintered alloys has been presented in this work. The model takes into account the heterogeneities of the structure due to porosity and the consequent stress concentrations and is based on the application of the Cell Method, a numerical method that is particularly suitable for heterogeneous materials. The development of plane models in the elastic and plastic field, also introduced in the paper, allowed to predict the behaviour of four sintered alloys, obtained from two different base materials at different porosity levels in a very good agreement with experimental data.

Acknowledgement: The financial support by the Italian Ministry of Research and University is acknowledged, under grant (PRIN 2007). The author wishes to express her appreciation to Prof. L. Bertini, Prof. V. Fontanari and Prof. G. Straffellini for sharing their files from experimental tests, to Prof. E. Tonti, University

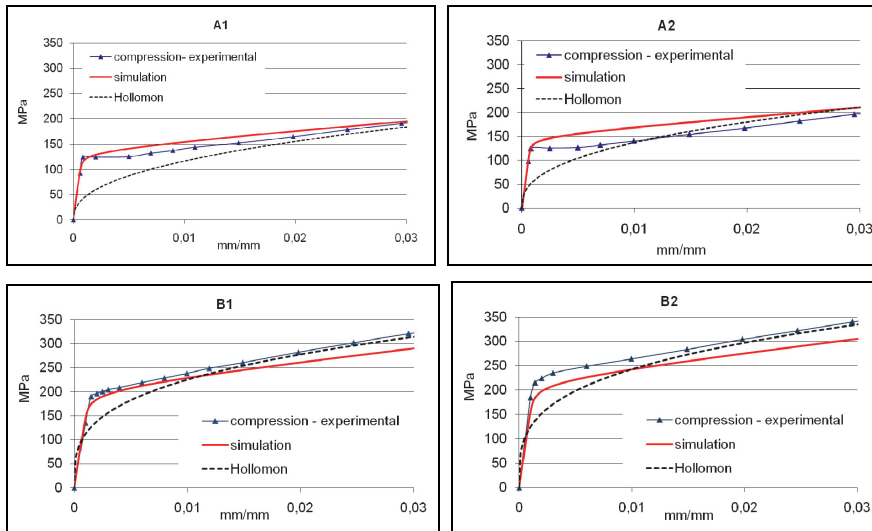


Figure 10: Stress/strain plot for alloy A1, A2, B1, B2: comparison among simulation, experimental test and Hollomon's approximation data.

of Trieste, to whom the Cell Method is due and to Prof. F. Miani, University of Udine, for helpful discussions on sintered materials.

References

- Alotto P., Gruosso G., Moro F., Repetto M.** (2008): A Boundary Integral Formulation for eddy current problems based on the Cell Method, *IEEE Trans. Magnetics*, vol. 44, pp.770-773.
- Bertini L., Fontanari V., Straffellini G.** (1998): Tensile and bending behavior of sintered alloys: experimental results and modeling. *J. of Engineering Materials and Technology*, vol. 120, pp. 248–255.
- Cannillo V., Carter, W. C.** (2000): Computation and Simulation of Reliability Parameters and their Variations in Heterogeneous Materials, *Acta Materialia*; vol. 48, pp. 3593-3605.
- Chao H., Bai J. and Ghosh S.** (2007): Micromechanical and macroscopic models of ductile fracture in particle reinforced metallic materials, *Modelling Simul. Mater. Sci. Eng.*, vol. 15, pp. S377-392.
- Codecasa L., Trevisan F.** (2006): Piecewise uniform bases and energetic approach for discrete constitutive matrices in electromagnetic problems, *Int. J. Numerical*

Methods in Engineering, vol. 65, n. 4, pp. 548-565.

Cosmi F. (2001): Numerical solution of Plane Elasticity Problems with the Cell Method, *CMES: Computer Modeling in Engineering & Sciences*, vol.2, n.3, pp. 365-372

Cosmi F. (2004): Two-dimension estimate of effective properties of solid with random voids, *Theoretical and Applied Fracture Mechanics*, vol.42, n.2, pp. 183-186

Cosmi F. (2005): Elastodynamics with the Cell Method, *CMES: Computer Modeling in Engineering & Sciences*, vol.8, n.3, pp. 191-200

Cosmi F. (2008): Dynamical Analysis of Mechanical Components: A Discrete Model for Damping, *CMES: Computer Modeling in Engineering & Sciences*, vol. 27, n. 3, pp.187-195.

Cosmi F. (2009): Morphology-based prediction of elastic properties of trabecular bone samples, *Acta of Bioengineering and Biomechanics*, vol.11, n.1, pp. 3-9

Cosmi F. (2011): Local anisotropy and elastic properties in a short glass fibre reinforced polymer composite, *Strain*, vol. 47, pp. 215–221

Cosmi F., Dreossi D. (2007a): Numerical and experimental structural analysis of trabecular architectures, *Meccanica*, vol. 42, n. 1, pp.85-93.

Cosmi F., Dreossi D. (2007b): The Application of the Cell Method for the Clinical Assessment of Bone Fracture Risk, *Acta of Bioengineering and Biomechanics*, vol. 9, n. 2, pp.35-39.

Cosmi F., Hoglevina M. (2010): An Application of the Cell Method to Multiaxial Fatigue Assessment of a Test Component under Different Criteria, *Strain*, vol. 46, n. 2, pp. 148–158.

Cosmi F., Steimberg N., Dreossi D., Mazzoleni G. (2009): Structural analysis of rat bone explants kept in vitro in simulated microgravity conditions, *J. Mechanical Behavior of Biomedical Materials*, vol.2 n.2, pp. 164-172.

Ferretti E. (2009): Cell Method Analysis of Crack Propagation in Tensioned Concrete Plates. *CMES: Computer Modeling in Engineering & Sciences*, vol. 54, pp. 253-282.

Ferretti E., Casadio E., Di Leo A. (2008): Masonry Walls under Shear Test: a CM Modeling, *CMES: Computer Modeling in Engineering & Sciences*, vol. 30, n. 3, pp.163-190.

Ghosh S., Mukhopadhyay S.N. (1991): A two-dimensional automatic mesh generator for finite element analysis for random composites, *Computers & Structures*, vol. 41, n. 2, pp. 245-256.

- Ghosh S.** (2004): Computational material modeling: a current perspective, *CMES: Computer Modeling in Engineering & Sciences*, vol. 5, n. 1, pp.1-3.
- Grujicic M., Zhang Y.** (1998): Determination of effective elastic properties of functionally graded materials using Voronoi cell finite element method, *Material science & engineering A* 251, pp. 64-76
- Heshmatzadeh M., Bridges G.E.** (2007): A Geometrical Comparison between Cell Method and Finite Element Method in Electrostatics, *CMES: Computer Modeling in Engineering & Sciences*, vol. 18, no. 1, pp.45-58.
- Nappi A, Rajgelj S, Zaccaria D.** (2001): Application of the Cell Method to Elastic-Plastic Analysis, in *Physics and Mechanics of Finite Plastic & Viscoplastic Deformation* edited by Akhtar S. Khan NEAT PRESS, Fulton, Mariland.
- Straface S., Troisi S., Gagliardi V.** (2006): Application of the Cell Method to the Simulation of Unsaturated Flow, *CMC: Computers, Materials and Continua*, vol.3, n.3, pp. 255-166.
- Taddei F., Pani M., Zovatto L., Tonti E., Viceconti M.** (2008): A new meshless approach for subject-specific strain prediction in long bones: Evaluation of accuracy, *Clinical Biomechanics*, vol. 23, pp.1192-1199.
- Tonti E., Zarantonello F.** (2010): Algebraic Formulation of Elastodynamics: the Cell Method, *CMES: Computer Modeling in Engineering & Sciences*, vol. 64, n.1, pp. 37-70.
- Tonti, E.** (2001): A Direct Discrete Formulation of Field Laws: The Cell Method, *CMES: Computer Modeling in Engineering & Sciences*, vol. 2, n.2, pp. 237-258.
- Zohdi T.D., Wriggers, P.** (2001): Computational Micro-macro Material Testing *Archives of Computational Methods in Engineering*; vol. 8, pp.131-228
- Zovatto L., Nicolini M.** (2007): Improving the Convergence Order of the Meshless Approach for the Cell Method for Numerical Integration of Discrete Conservation Laws, *Int. J. Computational Methods in Engineering Science and Mechanics*, vol. 8, n.5, pp. 273-281.
- Zovatto L., Nicolini, M.** (2006): Extension of the Meshless Approach for the Cell Method to Three-Dimensional Numerical Integration of Discrete Conservation Laws, *Int. J. Computational Methods in Engineering Science and Mechanics*, vol. 7, n.2, pp. 69-79.